

Fast Newton method solving KLR based on Multilevel Circulant Matrix with log-linear complexity

Junna Zhang¹, Shuisheng Zhou^{1*}, Cui Fu¹ and Feng Ye¹

^{1*}School of Mathematics and Statistics, Xidian University, Xi'an, 710126, China.

*Corresponding author(s). E-mail(s): sszhou@mail.xidian.edu.cn;

Contributing authors: junnazhang@stu.xidian.edu.cn; cufu@stu.xidian.edu.cn;
fye@xidian.edu.cn;

Abstract

Kernel logistic regression (KLR) is a conventional nonlinear classifier in machine learning. With the explosive growth of data size, the storage and computation of large dense kernel matrices is a major challenge in scaling KLR. Even the nyström approximation is applied to solve KLR, it also faces the time complexity of $O(\mathbf{nc}^2)$ and the space complexity of $O(\mathbf{nc})$, where \mathbf{n} is the number of training instances and \mathbf{c} is the sampling size. In this paper, we propose a fast Newton method efficiently solving large-scale KLR problems by exploiting the storage and computing advantages of multilevel circulant matrix (MCM). Specifically, by approximating the kernel matrix with an MCM, the storage space is reduced to $O(\mathbf{n})$, and further approximating the coefficient matrix of the Newton equation as MCM, the computational complexity of Newton iteration is reduced to $O(\mathbf{n} \log \mathbf{n})$. The proposed method can run in log-linear time complexity per iteration, because the multiplication of MCM (or its inverse) and vector can be implemented the multidimensional fast Fourier transform (mFFT). Experimental results on some large-scale binary-classification and multi-classification problems show that the proposed method enables KLR to scale to large scale problems with less memory consumption and less training time without sacrificing test accuracy.

Keywords: Kernel logistic regression, Newton method, Large scale, Multilevel circulant matrix approximation

1 Introduction

Kernel logistic regression (KLR) is a log-linear model with direct probabilistic interpretation and can be naturally extended to multi-class classification problems [1]. It is widely used in many fields, including automatic disease diagnosis [2], detecting fraud [3], landslide susceptibility mapping [4], etc. But it is difficult to scale to large-scale problems due to its high space and time complexity. A key issue in extending KLR to large-scale problems is the storage and computation of the kernel matrix, which is usually intensive. In particular,

when Newton method is used to solve KLR, the inverse operation of the Hessian matrix in each iteration requires $O(n^3)$ time and requires $O(n^2)$ space to store the kernel matrix.

A number of researchers have been working to make KLR feasible for large-scale problems [5, 6, 7]. They mainly start from the following two aspects: sparsity of solutions or decomposing the original problem into subproblems. Inspired by the sparsity of support vector machine (SVM), Zhu and Hastie [5] proposed the import vector machine (IVM) algorithm to reduced the time complexity of the binary classification of KLR to $O(n^2 s^2)$,

where s is the number of import points. IVM is still difficult to calculate for large-scale problems although the complexity has been reduced. Inspired by sequence minimum optimization algorithm (SMO) solving SVM, Keerthi et al. [7] proposed a fast dual algorithm for solving KLR. By continuously decomposing the original problem into subproblems, the fast dual algorithm only updates two variables per iteration. However, the time cost of iteratively updating values in the fast dual algorithm is increased by the introduction of the kernel matrix calculation. In short, existing methods still make it difficult to scale KLR to large-scale problems.

In this paper, we focus on kernel approximation to accelerate large-scale KLR inspired by the excellent performance of kernel approximation in learning problems [8, 9, 10, 11]. A great deal of work has been done on kernel approximation. The commonly used kernel approximation methods include Nyström method [12, 13, 14, 15, 16, 17], random feature [18, 19, 20, 21, 22, 23, 24, 25, 26], multilevel circulant matrix (MCM) [27, 28, 29, 30, 31, 32], and so on.

Nyström method is the classical kernel matrix approximation, whose outstanding feature is the sampling of data before large-scale matrix operations. After the Nyström method successfully and efficiently solves large-scale Gaussian processes [8], a number of sampling methods with strong theoretical guarantees have been proposed to satisfy the desired approximation with fewer sampling points. Among these sampling methods, the leverage score sampling technique [14] is the most widely used in practical applications. Recursive ridge leverage scores (RRLS) [15] finds a more accurate kernel approximation in less time by employing a fast recursive sampling scheme. However, in [33] the authors pointed out that the Nyström approximation is very sensitive to inhomogeneities in the sample.

The random feature is constructed randomly from a nonlinear mapping of the input space to the Hilbert space, that is, the direct approximation of the kernel function without calculating the elements in the kernel matrix. Rahimi and Recht [18] proposed the random feature map of shifted invariant kernel functions based on Fourier transform. In order to speed up feature projection,

Feng et al. [21] proposed structured random matrices, signed Circulant Random Matrix (CRM), to project input data. The feature mapping can be done in $O(nD \log d)$ time by using the fast Fourier Transform (FFT), where d and D represent the dimensions of the input data and the random feature space, respectively. Li et al. [25] provided the first unified risk analysis of learning with random Fourier features and proposed leverage score random feature mapping which needs $O(nD^2 + D^3)$ time to generate refined random features. Obviously, when d or D is very large, the feature mapping is costly.

The idea of MCM approximate kernel matrix was first proposed by Song and Xu [28] and many theoretical results are proven. By approximated the kernel matrix with MCM, researchers have developed many applications in different machine learning areas, such as the kernel ridge regression [30], automatic kernel selection problem [31] and least squares support vector machines [32], where the approximated kernel matrix is stored in $O(n)$ and the computational complexity of the corresponding algorithms is only $O(n \log n)$. Since MCM can save a lot of memory and has certain computing advantages, we choose MCM approximation to speed up KLR.

In the works [30, 31, 32], the core problem is to solve a system of linear equations $(\mathbf{K} + n\lambda\mathbf{I})\mathbf{d} = \mathbf{b}$, where \mathbf{K} is a kernel matrix or the linear combination of multiple kernel matrices and λ is the regularized parameter. If \mathbf{K} is approximated by an MCM, then $(\mathbf{K} + n\lambda\mathbf{I})$ is MCM too, hence the system of linear equations can be solved in $O(n \log n)$ time by the multidimensional fast Fourier transform (mFFT) owing to the advantages of MCM. When applying MCM directly to KLR, it faces to solve a system of linear equations $(\mathbf{K}^\top \mathbf{\Lambda} \mathbf{K} + n\lambda\mathbf{K})\mathbf{d} = \mathbf{b}$. Only approximated \mathbf{K} as an MCM, the coefficient matrix of the system of linear equations is still not an MCM. Hence it cannot be solved in $O(n \log n)$ and still suffers from high computational complexity. In this case, the most efficient scheme to solve it is to run conjugate gradient method T loops with the computational complexity $O(Tn \log n)$. Since $T = O(n)$ for conjugate gradient method [34], this scheme is still insufferable for large-scale problems.

In this work, to effectively solve KLR with large-scale training samples, we firstly simplify

the resulted Newton equation, then approximate the kernel matrix by MCM as [30, 31, 32] did. Further we approximate the coefficient matrix of the simplified Newton equation as an MCM too. Hence, we propose a fast Newton method based on MCM which can efficient solve large-scale KLR with $O(n)$ space complexity and $O(n \log n)$ computational complexity. Many experimental results support that the proposed method can make KLR problem scalable.

The rest of the paper is organized as follows. In Section 2, we review KLR and MCM. In Section 3, we present the fast Newton method based on MCM approximation for solving KLR. We report experimental results in Section 4. Section 5 concludes this paper.

2 Preliminaries

In this section, we review KLR and MCM and introduce some interesting properties of MCM.

2.1 Kernel Logistic Regression

Given the training set $\mathbb{D} = \{(\mathbf{x}_i, \mathbf{y}_i), i = 1, \dots, n\}$, where $\mathbf{x}_i \in \mathcal{X} \in \mathbb{R}^d$ is the input data and $\mathbf{y}_i \in \{0, 1\}$ is the output targets corresponding to the input. A reproducing kernel Hilbert space \mathbb{H} is defined by a kernel function $\kappa(\mathbf{x}, \mathbf{z}) = \langle \varphi(\mathbf{x}), \varphi(\mathbf{z}) \rangle$ with $\varphi : \mathbb{R}^d \mapsto \mathbb{H}$, which measures the inner product between the input vectors in the feature space. Then a traditional logistic regression model [35] is constructed in the feature space as follows

$$\min_{\mathbf{w} \in \mathbb{H}} \frac{\lambda}{2} \|\mathbf{w}\|^2 - \frac{1}{n} (\mathbf{y}^\top \ln \mathbf{p} + (\mathbf{1} - \mathbf{y})^\top \ln(\mathbf{1} - \mathbf{p})), \quad (1)$$

where $\mathbf{p}_i = 1/(1 + e^{-\langle \mathbf{w}, \varphi(\mathbf{x}_i) \rangle})$ is the posterior probability estimation of $\mathbf{y}_i = 1$, $\lambda > 0$ is the regularization parameter, and $\mathbf{1}$ is the all-one vector.

By the representer theorem [36], the solution to the optimization problem (1) can be represented as

$$\mathbf{w} = \sum_{i=1}^n \alpha_i \varphi(\mathbf{x}_i), \quad (2)$$

where $\alpha \in \mathbb{R}^n$. Then plugging (2) in (1), we can get the following KLR model

$$\min_{\alpha \in \mathbb{R}^n} F(\alpha) = \frac{\lambda}{2} \alpha^\top \mathbf{K} \alpha - \frac{1}{n} (\mathbf{y}^\top \ln \mathbf{p} + (\mathbf{1} - \mathbf{y})^\top \ln(\mathbf{1} - \mathbf{p})), \quad (3)$$

where \mathbf{K} is the kernel matrix satisfying $\mathbf{K}_{i,j} = \kappa(\mathbf{x}_i, \mathbf{x}_j)$, $\mathbf{p}_i = 1/(1 + e^{-\mathbf{K}(i,\cdot)\alpha})$, and $\mathbf{K}(i,\cdot)$ denotes the i -th row of the kernel matrix.

KLR is a convex optimization problem, which can be solved by Newton method [37] with quadratic convergence rate. However, Newton method requires $O(n^3)$ time complexity and $O(n^2)$ space complexity for each iteration, which is not feasible for large-scale data sets. Therefore, we need a more effective method to solve KLR.

2.2 Multilevel Circulant Matrix Approximation

Here we introduce the concept of MCM and some of its interesting properties, and analyze its computational advantages.

To facilitate representation, we introduce the notion of multilevel indexing [28]. In order to construct a q -level circulant matrix of level order \mathbf{q} , it is necessary to decompose $n \in \mathbb{N}$ into the product of $q \in \mathbb{N}$ positive integers, that is, $n = n_0 n_1 \cdots n_{q-1}$. We denote $\mathbf{q} := [n_0, n_1, \dots, n_{q-1}] \in \mathbb{N}^q$. Then, multilevel indexing $[\mathbf{q}]$ of the q -level circulant matrix is defined as follows

$$[\mathbf{q}] := [n_0] \times [n_1] \times \cdots \times [n_{q-1}] \in \mathbb{R}^{n \times q},$$

(Cartesian product)

where $[n_{q-j}] := \{0, 1, \dots, n_{q-j}\}$, $j = 1, 2, \dots, q$.

According to [38], if a matrix $\mathbf{K}_{\mathbf{q}}$ consists of $n_0 \times n_0$ blocks and each block $(q-1)$ -level circulant matrix of level order $[n_1, \dots, n_{q-1}]$, then $\mathbf{K}_{\mathbf{q}}$ is called a q -level circulant matrix. In other words, an MCM is a matrix that can be partitioned into blocks, which are further partitioned into smaller blocks. Specifically, $\mathbf{K}_{\mathbf{q}} = [\mathbf{K}_{i,j} : \mathbf{i}, \mathbf{j} \in [\mathbf{q}]]$ is called a q -level circulant matrix if for any $\mathbf{i} = (i_0, i_1, \dots, i_{q-1}) \in [\mathbf{q}]$, $\mathbf{j} = (j_0, j_1, \dots, j_{q-1}) \in [\mathbf{q}]$,

$$\mathbf{K}_{i,j} = \mathbf{k}_{i_0 - \text{mod}(j_0, n_0), \dots, i_{q-1} - \text{mod}(j_{q-1}, n_{q-1})},$$

where \mathbf{k} is the first column of $\mathbf{K}_{\mathbf{q}}$. Then a q -level circulant matrix $\mathbf{K}_{\mathbf{q}}$ is fully determined by its first column. So we write $\mathbf{K}_{\mathbf{q}} = \text{circ}_{\mathbf{q}}[\mathbf{k}]$.

The computational advantages of MCM are analyzed in detail in [39], and the key conclusions are restated as follows.

Lemma 1. [39] *Suppose that \mathbf{K}_q is an MCM of level order q and \mathbf{k} is its first column. Then \mathbf{K}_q is a q -level circulant matrix of level order q if and only if*

$$\mathbf{K}_q = \frac{1}{n} \phi^* \text{diag}(\phi \mathbf{k}) \phi, \quad (4)$$

where $\phi = \mathbf{F}_{n_0} \otimes \mathbf{F}_{n_1} \otimes \cdots \otimes \mathbf{F}_{n_{q-1}}$, $\mathbf{A} \otimes \mathbf{B}$ denotes the Kronecker product of \mathbf{A} and \mathbf{B} , and $\mathbf{F}_{n_{q-j}} = [e^{(2\pi i/n_{q-j})st} : s, t \in [n_{q-j}]]$, $j = 1, 2, \dots, q$ with i being the imaginary unit.

Theorem 1. [39] *Assume that \mathbf{A}_q and \mathbf{B}_q are both MCM of level order q , then $\mathbf{A}_q + \mathbf{B}_q$ is also an MCM of level order q .*

Theorem 2. [39] *Assume that \mathbf{A}_q is an invertible MCM of level order q and \mathbf{a} is the first column of \mathbf{A}_q , $\boldsymbol{\nu} = \phi \mathbf{a}$ is the vector of eigenvalues, then \mathbf{A}_q^{-1} is also an MCM, and $\mathbf{A}_q^{-1} = (1/n) \phi^* (\text{diag}(\boldsymbol{\nu}))^{-1} \phi$.*

The following Algorithm 1 proposed in [27] can construct an MCM \mathbf{K}_q from a kernel function to approximate the kernel matrix \mathbf{K} .

Algorithm 1 Construction of an MCM [27]

Input: a kernel function κ , a sequence of positive numbers $\mathbf{h} = (\mathbf{h}_0, \mathbf{h}_1, \dots, \mathbf{h}_{q-1}) \in \mathbb{R}^q$, level order $q \in \mathbb{N}^q$.

Output: \mathbf{K}_q .

- 1: Calculate $\mathbf{t}_i = \kappa(\| [i_s \mathbf{h}_s : s \in [q]] \|_2)$, $\forall i \in [q]$.
 - 2: Let $\mathbf{D}_{i,s} = \begin{cases} \{0\}, & \mathbf{i}_s = 0, \\ \{\mathbf{i}_s, \mathbf{q}_s - \mathbf{i}_s\}, & 1 \leq \mathbf{i}_s \leq \mathbf{q}_s - 1, \end{cases}$
and $\mathbf{D}_i = \mathbf{D}_{i,0} \times \mathbf{D}_{i,1} \times \cdots \times \mathbf{D}_{i,q-1}$, $\forall i \in [q]$
and $\forall s \in [q]$.
 - 3: Calculate $\mathbf{k}_i = \sum_{j \in \mathbf{D}_i} \mathbf{t}_j$.
 - 4: **return** $\mathbf{K}_q = \text{circ}_q[\mathbf{k}]$.
-

For \mathbf{K}_q generated by Algorithm 1, only $O(n)$ is required to store it since we only need to store the first column. By Lemma 1, $\mathbf{K}_q \mathbf{x}$ is equivalent to implementing $(1/n) \phi^* \text{diag}(\phi \mathbf{k}) \phi \mathbf{x}$, which can be realized efficiently in $O(n \log n)$ using the

mFFT. According to Theorem 2, $\mathbf{K}_q^{-1} \mathbf{x}$ is equivalent to implementing $(1/n) \phi^* (\text{diag}(\phi \mathbf{k}))^{-1} \phi \mathbf{x}$, which also can be realized efficiently in $O(n \log n)$. In addition to its advantages in computation and space storage, MCM approximation also does not require any sampling techniques. Next, we will design a fast and effective method to solve KLR based on MCM.

3 Fast Newton Method Based on MCM Approximation

In this section, we first simplify the Newton equation of KLR, then approximate the coefficient matrix of the simplified Newton equation as an MCM, finally propose a fast Newton method based on MCM approximation.

3.1 Simplify the Newton equation

KLR is a convex optimization problem [40], and the local optimal solution must be the global optimal solution. For convex optimization issues, Newton method with at least quadratic convergence can be used to solve them. The gradient and Hessian are obtained by differentiating (3) with respect to $\boldsymbol{\alpha}$. The gradient is

$$\nabla F(\boldsymbol{\alpha}) = \lambda \mathbf{K} \boldsymbol{\alpha} - \frac{1}{n} \mathbf{K}(\mathbf{y} - \mathbf{p}), \quad (5)$$

and the Hessian of (3) is

$$\nabla^2 F(\boldsymbol{\alpha}) = \frac{1}{n} \mathbf{K}^\top \boldsymbol{\Lambda} \mathbf{K} + \lambda \mathbf{K}, \quad (6)$$

where $\boldsymbol{\Lambda}$ is a diagonal matrix with $\boldsymbol{\Lambda}_{ii} = \mathbf{p}_i(1 - \mathbf{p}_i)$. Based on the (5) and (6), we need to solve the following Newton equation

$$\left(\mathbf{K}^\top \boldsymbol{\Lambda} \mathbf{K} + n \lambda \mathbf{K} \right) \mathbf{d} = \mathbf{K}(\mathbf{y} - \mathbf{p} - n \lambda \boldsymbol{\alpha}), \quad (7)$$

to update the current solution. Obviously, in order to compute the Newton direction \mathbf{d} , the computational complexity is $O(n^3)$ per iteration, which is prohibitively expensive for large-scale problems. In order to reduce the computational cost, we first simplify the Newton equation. Since the kernel matrix is symmetric, we have

$$\mathbf{K}(\boldsymbol{\Lambda} \mathbf{K} + n \lambda \mathbf{I}) \mathbf{d} = \mathbf{K}(\mathbf{y} - \mathbf{p} - n \lambda \boldsymbol{\alpha}). \quad (8)$$

If the kernel matrix K is positive definite, we can simplify (8) as

$$(\mathbf{\Lambda}K + n\lambda\mathbf{I})\mathbf{d} = \mathbf{y} - \mathbf{p} - n\lambda\boldsymbol{\alpha}. \quad (9)$$

If the kernel matrix K is positive semidefinite, then the solution to (8) is not necessarily unique, but the unique solution of (9) is the solution of (8). Therefore, we can use the solution of (9) as the Newton direction.

Replacing K in (9) with K_q generated by Algorithm 1, we can further obtain the following approximated Newton equation

$$(\mathbf{\Lambda}K_q + n\lambda\mathbf{I})\bar{\mathbf{d}} = \mathbf{y} - \bar{\mathbf{p}} - n\lambda\boldsymbol{\alpha}, \quad (10)$$

where $\bar{p}_i = 1/(1 + e^{-K_q(i,\cdot)\boldsymbol{\alpha}})$ and $K_q(i, \cdot)$ is the i -th row of K_q .

If solving (10) by the conjugate gradient method [34] to obtain an approximated Newton direction, the time complexity of each iteration is $O(n \log n)$ due to the use of mFFT.

In this case, the most efficient scheme to solve (10) is to run conjugate gradient method T loops with the computational complexity $O(Tn \log n)$. Since $T = O(n)$ for conjugate gradient method [34], this scheme is still insufferable for large-scale problems. Then we expect to find a more efficient way to calculate the Newton direction.

3.2 Approximate the Coefficient Matrix of Newton Equation using MCM

In this section, we approximate the coefficient matrix of equation (10) as an MCM, then we can calculate the Newton direction more efficiently.

According to Theorem 2, if we can approximate $\mathbf{\Lambda}K_q + n\lambda\mathbf{I}$ with an MCM, then we can directly calculate $\bar{\mathbf{d}}$ in $O(n \log n)$ time by using mFFT. Obviously, we only need to approximate $\mathbf{\Lambda}K_q$ since $n\lambda\mathbf{I}$ is already an MCM. To this end, we solve the least squared problem

$$\min_{\mathbf{A}_q \in \mathbb{A}_q} \|\mathbf{\Lambda}K_q - \mathbf{A}_q\|_F^2, \quad (11)$$

where \mathbb{A}_q is the set of MCM of level order q . Here we use the Frobenius Norm for simplicity, and the other norms of matrix can be used.

By working out the optimality condition of the problem (11), we obtain the following proposition.

Proposition 1. *The optimal solution of the problem (11) is*

$$\mathbf{A}_q = \tau\mathbf{K}_q, \quad (12)$$

where $\tau = (1/n) \sum_{i=1}^n \mathbf{\Lambda}_{ii}$.

Proof Let \mathbf{k} be the first column of K_q and \mathbf{a} be the first column of A_q , where $\mathbf{k} = (\mathbf{k}_1, \mathbf{k}_2, \dots, \mathbf{k}_n)$ and $\mathbf{a} = (\mathbf{a}_1, \mathbf{a}_2, \dots, \mathbf{a}_n)$. According to the built-in periodicity of K_q and A_q , the problem (11) is equivalent to

$$\min_{\mathbf{a}_j \in \mathbb{R}} \sum_{i=1}^n \sum_{j=1}^n (\mathbf{\Lambda}_{ii}\mathbf{k}_j - \mathbf{a}_j)^2. \quad (13)$$

The first-order optimality conditions of the problem (13) is

$$\sum_{i=1}^n (\mathbf{\Lambda}_{ii}\mathbf{k}_j - \mathbf{a}_j) = 0, j = 1, 2, \dots, n.$$

Hence, the optimal solution of the problem (13) is

$$\mathbf{a}_j = \frac{1}{n} \sum_{i=1}^n \mathbf{\Lambda}_{ii}\mathbf{k}_j, j = 1, 2, \dots, n.$$

Thus the optimal solution of the problem (11) is (12), which proves the proposition. \square

According to Proposition 1, we replace $\mathbf{\Lambda}K_q$ in (10) with $\mathbf{A}_q = \tau\mathbf{K}_q$, and get the following equation

$$(\tau\mathbf{K}_q + n\lambda\mathbf{I})\tilde{\mathbf{d}} = \mathbf{y} - \tilde{\mathbf{p}} - n\lambda\boldsymbol{\alpha}, \quad (14)$$

where $\tilde{p}_i = 1/(1 + e^{-K_q(i,\cdot)\boldsymbol{\alpha}})$.

Then, we can obtain the following approximate Newton direction

$$\tilde{\mathbf{d}} = \frac{1}{\tau}(\mathbf{K}_q + \tilde{\tau}\mathbf{I})^{-1}(\mathbf{y} - \tilde{\mathbf{p}} - n\lambda\boldsymbol{\alpha}), \quad (15)$$

where $\tilde{\tau} = n\lambda/\tau$.

According to the nice properties of MCM, the cost of calculating the approximated Newton direction (15) is $O(n \log n)$, which is much less than $O(n^2 \log n)$ and $O(n^3)$.

To illustrate the effectiveness of using the approximated Newton direction (15), we compare the fast Newton method based on MCM approximation with the Newton method based on (9) and the Newton method based on (10) experimentally. A 2-dimensional separable dataset for nonlinear classification was randomly sampled, which comprised 3375 training samples and 625 test samples. The training samples of class 1 are plotted as light-skyblue plus (+), and the training samples of class

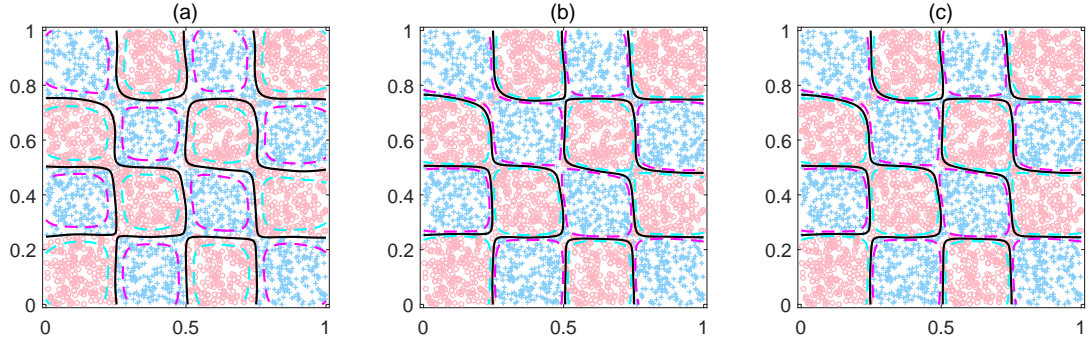


Fig. 1: Nonlinear classification experiments. (a) Newton method based equation (9). (b) Newton method based equation (10). (c) Newton method based equation (15). The training samples of class 1 are plotted as lightskyblue plus (+), and the training samples of class 0 are plotted as lightpink circle (◐). The solid black lines are the classification boundaries; the cyan dashed line and the magenta dashed line are the lines with predicted probabilities of 0.25 and 0.75, respectively. The test accuracies for the corresponding methods are 0.9585, 0.9584 and 0.9584 on 625 test samples, and the training time for the corresponding methods are 109.63s, 7.49s and 0.05s on 3375 train samples.

0 are plotted as lightpink circle (◐). The solid black lines are the classification boundaries; the cyan dashed line and the magenta dashed line are the lines with predicted probabilities of 0.25 and 0.75, respectively (Fig. 1).

In Fig. 1, it can be seen that the classification boundaries of the three Newton methods are almost the same. From the contour line of the predicted probability, the first method has more samples with the predicted probability between 0.25 and 0.75 than the latter two methods. The test accuracies for the corresponding methods are 0.9585, 0.9584 and 0.9584 on 625 test samples, and the training time for the corresponding methods are 109.63s, 7.49s and 0.05s on 3375 train samples. This validates the efficiency of the fast Newton method based on the MCM approximation.

3.3 Fast Newton Method

We are now ready to develop a fast Newton method based on MCM approximation, which can reduce the time and space complexity more succinctly and effectively.

The main work of Newton method is the calculation of Newton direction. According to Theorem 1, $\mathbf{K}_q + \tilde{\tau}\mathbf{I}$ is an MCM. By Theorem 2, we have

$$(\mathbf{K}_q + \tilde{\tau}\mathbf{I})^{-1} = \frac{1}{n} \phi^* (\text{diag}(\mathbf{v} + \tilde{\tau}\mathbf{1}))^{-1} \phi,$$

where $\mathbf{v} = \phi\mathbf{k}$ is the vector of eigenvalues.

Then we rewrite (15) as follows:

$$\tilde{\mathbf{d}} = \frac{1}{n\tau} \phi^* (\text{diag}(\mathbf{v} + \tilde{\tau}\mathbf{1}))^{-1} \phi (\mathbf{y} - \tilde{\mathbf{p}} - n\lambda\boldsymbol{\alpha}). \quad (16)$$

In addition, replacing \mathbf{K} with \mathbf{K}_q generated by Algorithm 1, we note the approximations of the objective function (3) and its gradient (5) as follows.

$$\tilde{F}(\boldsymbol{\alpha}) = \frac{\lambda}{2} \boldsymbol{\alpha}^\top \mathbf{K}_q \boldsymbol{\alpha} - \frac{1}{n} (\mathbf{y}^\top \ln \tilde{\mathbf{p}} + (\mathbf{1} - \mathbf{y})^\top \ln(\mathbf{1} - \tilde{\mathbf{p}})), \quad (17)$$

$$\nabla \tilde{F}(\boldsymbol{\alpha}) = \mathbf{K}_q (\lambda \boldsymbol{\alpha} - \frac{1}{n} (\mathbf{y} - \tilde{\mathbf{p}})). \quad (18)$$

Now we present the detailed flow of the Fast Newton method based on MCM approximation in Algorithm 2.

3.4 Complexity Analysis

Due to the nice properties of MCM, our algorithm can reduce the time complexity and space complexity in solving KLR more succinctly. In the following, we will study the time and space complexity of the Algorithm 2 in more detail.

Space Complexity. Because of the built-in periodicity of MCM, only $O(n)$ space storage is required. This plays an important role in the consumption of memory. Considering the fragmentation memory footprint of the other parameters, we can eventually abbreviate the space complexity of the Algorithm 2 to $O(n)$.

Algorithm 2 Fast Newton method based on MCM

Input: Training set \mathbb{D} , parameters $\sigma, \lambda, T, \varepsilon, \delta \in (0, 1)$, $\beta \in (0, 0.5)$ and given an initial α_0 .

Output: α .

- 1: Calculate $[k_i : i \in [q]]$ according to Algorithm 1.
 - 2: Calculate $\mathbf{v} = \phi[k_i : i \in [q]]$ by mFFT.
 - 3: Calculate $\tilde{\mathbf{p}}, \nabla \tilde{F}(\alpha_0)$ and $\tilde{F}(\alpha_0)$.
 - 4: **while** $t \leq T_{max}$ and $\nabla \tilde{F}(\alpha_t) > \varepsilon$ **do**
 - 5: Calculate $\boldsymbol{\eta} = (1/\tau)(\mathbf{y} - \tilde{\mathbf{p}} - n\lambda\alpha_t)$.
 - 6: Calculate $\boldsymbol{\delta} = \phi\boldsymbol{\eta}$ by mFFT.
 - 7: Calculate $\boldsymbol{\zeta} = (\text{diag}(\mathbf{v} + \tilde{\tau}\mathbf{1}))^{-1}\boldsymbol{\delta}$.
 - 8: Calculate $\tilde{\mathbf{d}} = \frac{1}{n}\phi^*\boldsymbol{\zeta}$ using inverse mFFT.
 - 9: (Armijo line search [41]) Set $r_t = \delta^{m_t}$, where m_t is the first nonnegative integer m for which

$$\tilde{F}(\alpha_t + \delta^m \tilde{\mathbf{d}}) \leq \tilde{F}(\alpha_t) + \beta \delta^m \langle \nabla \tilde{F}(\alpha_t), \tilde{\mathbf{d}} \rangle.$$
 - 10: Update $\alpha_{t+1} = \alpha_t + r_t \tilde{\mathbf{d}}$, calculate $\tilde{\mathbf{p}}$ and $\nabla \tilde{F}(\alpha_{t+1})$.
 - 11: $t := t + 1$.
 - 12: **end while**
 - 13: **return** $\alpha \leftarrow \alpha_t$.
-

Time Complexity. From [30], the complexity of the step 1 is $O(n)$. We know the computational complexity of steps 2, 6 and 8 is $O(n \log n)$, since mFFT can be applied with the $O(n \log n)$ complexity. The main work of the steps 3 and 10 is to calculate the form $K_q \mathbf{x}$. According to Section 2.2, the computational complexity of the steps 3 and 10 is $O(n \log n)$. The computational complexity of the step 7 is $O(n)$. In the process of calculating $\tilde{F}(\alpha_t + \delta^m \tilde{\mathbf{d}})$ in the step 9, we can store $K_q \alpha_t$ and $K_q \tilde{\mathbf{d}}$ to facilitate the calculation of $\tilde{F}(\alpha_t + \delta^m \tilde{\mathbf{d}})$. Then only $O(n)$ times multiplications are needed to calculate $\tilde{F}(\alpha_t + \delta^m \tilde{\mathbf{d}})$ in the step 9. If the number of iterations is $T \leq T_{max}$, the total maximum computational complexity of Algorithm 2 is $O(nq + Tn \log n)$. At the same time, [32] showed that a small q (e.g., 3) is sufficient for a sufficient approximation of the classification problem. This means that we can abbreviate the time complexity of the Algorithm 2 to $O(Tn \log n)$, where T is always less than 10 for the convex KLR problem.

We list the computational complexity and space complexity of several kernel approximation methods for solving KLR in Table 1.

Table 1: Compare the typical approximation methods of solving KLR by Newton method. The space complexity of every method is in the second column. The time complexity per iteration for each method is in the third column. n denotes the number of training data. d denotes the data dimension. c represents the sampling size. D denotes the dimensionality of the random feature space.

Method	Space complexity	Time complexity
Original	$O(n^2)$	$O(n^3 + n^2)$
Nys [8]	$O(nc)$	$O(nc^2 + nc + c^3)$
RRLS-Nys [14]	$O(nc)$	$O(nc^2 + nc + c^3)$
SCRf [21]	$O(nD)$	$O(nD^2 + nD \log d + D^3)$
LS-RFF [25]	$O(nD)$	$O(nD^2 + nD + D^3)$
Ours	$O(n)$	$O(n \log n)$

4 Experiment

In this section, we conduct experiments on some binary and multi-classification datasets to evaluate the effectiveness of our algorithm. All the experiments were in MATLAB and run on a 3.6 GHz Intel Core i7 with 16GB of memory.

4.1 Compared Methods and Parameter Settings

We compare our method with the following state-of-the-art kernel matrix approximation methods:

- Nys [8]: The standard form of Nyström method, whose sampling method uses uniform sampling.
- RRLS-Nys [14]¹: Recursive ridge leverage scores finds a more accurate kernel approximation in less time by employing a fast recursive sampling scheme.
- SCRf [21]: The transformation matrix is constructed by a signed Circulant Random Matrix (CRM) and the feature mapping can be done in $O(nD \log d)$ time by using the fast Fourier Transform (FFT).
- LS-RFF [25]²: The transformation matrix is constructed based on the leverage score, which takes $O(nD^2 + D^3)$ time to generate refined random features.

We fixed $T_{max} = 30$, and the stop criterion $\varepsilon = 10^{-5}$. The kernel function we use is $\kappa(\mathbf{x}, \mathbf{z}) = \exp(-\sigma \|\mathbf{x} - \mathbf{z}\|^2)$, where $\sigma > 0$ is the kernel parameter. For all the experiments, there are two parameters need to be determined in advance, i.e.,

¹Codes are available in <https://github.com/cnmusco/recursive-nyström>.

²Codes are available in <http://www.lfhsgr.org>.

σ and λ . The regularization parameter λ and the kernel parameter σ listed in Table 2 were chosen by a cross-validation procedure and grid search with $\sigma \in \{2^{-9}, \dots, 2^{16}\}$ and $\lambda \in \{10^{-6}, \dots, 10^0\}$.

Table 2: Parameter settings of algorithms.

Binary				Multi-class				
Data Sets	σ	λ	Data Sets	σ	λ	Data Sets	σ	λ
Ionosphere	2^2	10^{-3}	Adult	2^{-7}	10^{-3}	Shuttle	2^{15}	10^{-3}
Australian	2^{-7}	10^{-2}	Shuttle	2^{15}	10^{-3}	Sensorless	2^9	10^{-4}
Banknote	2^2	10^{-2}	Mnist	2^{-1}	10^{-5}	Connect-4	2^2	10^{-4}
Titanic	2^{-2}	10^{-1}	Vehicle	2^{-4}	10^{-1}	Mnist	2^{-1}	10^{-6}
Banana	2^3	10^{-3}	Skin	2^{11}	10^{-3}	Vehicle	2^5	10^{-3}
USPS	2^{-1}	10^{-4}	Covtype	2^9	10^{-4}	CovtypeM	2^9	10^{-4}

The sampling size c of the Nyström method and the recursive RLS-Nyström was set to $c = \sqrt{n}$. The dimensionality D of SCRF and LS-RFF was set to $D = O(d)$. For MCM approximation, a 3-level circulant matrix was adopted. In the experiments, we fix $\mathbf{h} = \mathbf{1} \in \mathbb{R}^q$, since it is sufficient to demonstrate the validity of the Algorithm 2. To avoid randomness, all experiments are operated 10 times independently, and the mean value is taken as the final result.

4.2 Small-scale Benchmark Datasets Experiments

In this section, we test six small-scale benchmark classification datasets to illustrate that the classification performance of the approximation algorithms is comparable to the original algorithm. For USPS, the task of classifying the digit 8 versus the rest classes was trained. The Australian and USPS datasets were downloaded from the LIBSVM [42], and the Ionosphere, Banknote, Titanic and Banana datasets were downloaded from the UCI database [43]. These datasets are detailed in Table 3.

The variation trend of the two-norm of the gradient with the number of iterations is plotted in Fig. 2. Table 3 reports the experimental results for the six small-scale datasets. The training time is not listed in Table 3, because the training time of these methods is very small.

It can be seen from Fig. 2 that, compared with the original algorithm, several approximation algorithms can converge, and at the same time, the

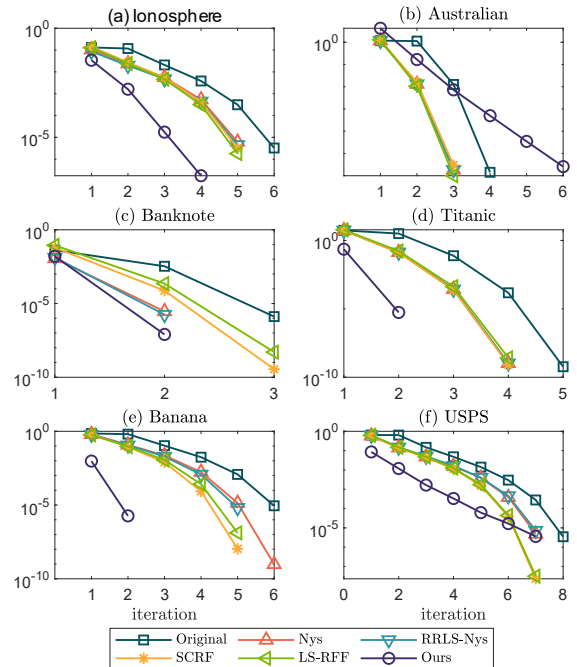


Fig. 2: Plots for the variation trend of the two-norm of the gradient with the number of iterations on the six small-scale benchmark classification datasets.

number of iterations when convergence is achieved will be reduced.

From Table 3, it is clear that the classification performance of the five approximation algorithms is comparable to that of the original algorithm.

4.3 Large-scale Benchmark Datasets Experiments

In this section, we test six large datasets of benchmark classification to further demonstrate the superiority of our algorithm. For Mnist, the task of classifying the digit 8 versus the rest classes was trained. For Vehicle, the task of classify class 3 from the rest was trained. These datasets were downloaded from the LIBSVM [42].

The variation trend of the two-norm of the gradient with the number of iterations is plotted in Fig. 3. Table 4 reports the experimental results for the six large-scale datasets.

From Fig. 3, the five approximation algorithms can reach convergence in six large-scale data sets. The convergence process of Nys and RRLS-Nys is basically the same. The convergence process of SCRF and LS-RFF is basically the same. Several

Table 3: Comparison of different algorithms on the six small-scale benchmark classification datasets. The standard deviations are given in brackets. 'AUC' stands for "Area under the ROC Curve". n and m are the numbers of training and testing samples respectively. d is the dimension of data.

Data Sets	Algorithms	Acc(%)	AUC(%)
Ionosphere n=216 m=135 d=34	Original	92.30	97.53(1.06)
	Nys	91.41	96.76(1.39)
	RRLS-Nys	91.41	97.71(1.13)
	SCRF	91.04	97.54(1.11)
	Ours	92.22	97.81(1.00)
Australian n=512 m=178 d=14	Original	85.11	92.74(2.16)
	Nys	84.89	91.89(1.80)
	RRLS-Nys	84.38	92.38(1.69)
	SCRF	84.27	92.22(1.79)
	Ours	87.64	92.54(2.19)
Banknote n=1000 m=372 d=4	Original	1.00	1.00(0.00)
	Nys	99.95	1.00(0.00)
	RRLS-Nys	99.95	1.00(0.00)
	SCRF	99.87	1.00(0.00)
	Ours	99.92	1.00(0.00)
Titanic n=1331 m=870 d=3	Original	77.41	74.75(1.00)
	Nys	77.48	74.06(1.47)
	RRLS-Nys	77.51	74.50(1.65)
	SCRF	77.15	73.65(1.99)
	Ours	77.31	73.58(1.05)
Banana n=3430 m=1870 d=2	Original	90.54	96.82(0.18)
	Nys	89.86	95.67(0.86)
	RRLS-Nys	89.78	95.98(0.35)
	SCRF	87.46	93.62(1.56)
	Ours	90.43	96.06(0.30)
USPS n=7291 m=2007 d=256	Original	99.26	98.95(0.14)
	Nys	99.25	98.83(0.24)
	RRLS-Nys	99.26	98.90(0.18)
	SCRF	99.23	98.89(0.21)
	Ours	99.25	98.90(0.25)
	Ours	99.13	99.33(0.14)

approximation methods can converge with very few iterations.

From Table 4, we have four observations. First, our algorithm's classification performance is comparable to the other four algorithms on all datasets except Vehicle. For Vehicle, the other four algorithms have slightly higher accuracy and AUC than our algorithm, but our algorithm has the least training time. Second, the performance of SCRf is slightly worse than that of Nys and RRLS-Nys, and the performance of Nys and

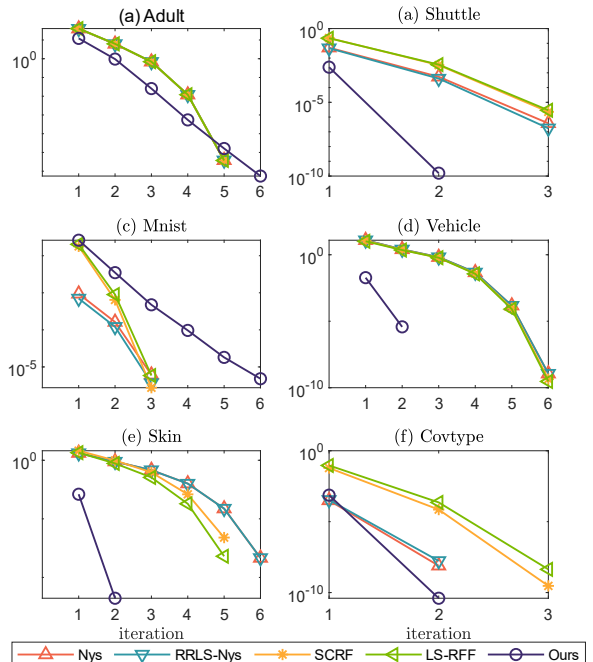


Fig. 3: Plots for the variation trend of the two-norm of the gradient with the number of iterations on the six large-scale benchmark classification datasets.

RRLS-Nys is similar, which is consistent with the conclusions of [15]. Third, the larger the dimension of training set is, the time cost of SCRf and LS-RFF increases obviously, which is consistent with the complexity analysis. Fourth, it can be clearly seen that the larger the training set is, the more obvious the efficiency gain of our algorithm is, which is consistent with the results of complexity analysis.

4.4 Checkerboard Dataset Experiments

In order to further illustrate the superiority of our algorithm, the influence of the sampling size of the Nys and RRLS-Nys on the classification performance of Checkerboard dataset is specifically analyzed in this section.

Checkerboard dataset was first proposed in [44] and later widely used to illustrate the effectiveness of nonlinear kernel method [45, 46, 47]. Checkerboard dataset was generated by the following method: randomly sampled 1,600,000 points from the regions $[0, 1] \times [0, 1]$ and labeled

Table 4: Comparison of different algorithms on the six large-scale benchmark classification datasets. 'AUC' stands for "Area under the ROC Curve". n and m are the numbers of training and testing samples respectively. d is the dimension of data. The standard deviations are given in brackets.

Data Sets	Algorithms	Training time(s)	Acc (%)	AUC (%)
Adult n=32,561 m=16,281 d=123	Nys	0.45(0.01)	81.79	88.39(0.00)
	RRLS-Nys	0.54(0.01)	81.82	88.39(0.01)
	SCRFF	5.35(0.17)	81.72	88.40(0.12)
	LS-RFF	5.96(0.06)	82.37	88.22(0.10)
	Ours	0.24(0.01)	82.08	86.55(0.02)
Shuttle n=43,500 m=14,500 d=9	Nys	0.54(0.03)	99.85	99.98(0.00)
	RRLS-Nys	0.89(0.07)	99.85	99.98(0.00)
	SCRFF	0.25(0.05)	99.84	99.97(0.00)
	LS-RFF	0.33(0.05)	99.84	99.98(0.00)
	Ours	0.32(0.02)	99.85	99.97(0.00)
Mnist n=60,000 m=10,000 d=784	Nys	1.20(0.04)	99.31	99.47(0.01)
	RRLS-Nys	2.45(0.06)	99.32	99.47(0.01)
	SCRFF	9.63(0.23)	99.29	99.46(0.00)
	LS-RFF	12.06(0.15)	99.30	99.47(0.00)
	Ours	0.46(0.01)	99.39	99.62(0.01)
Vehicle n=78,823 m=19,705 d=100	Nys	1.32(0.05)	85.37	91.44(0.00)
	RRLS-Nys	1.44(0.03)	85.38	91.45(0.00)
	SCRFF	7.70(0.16)	83.95	90.50(0.00)
	LS-RFF	6.64(0.09)	83.95	90.50(0.09)
	Ours	0.56(0.03)	83.92	87.11(0.03)
Skin n=157,464 m=87,593 d=3	Nys	9.30(0.21)	99.94	99.96(0.00)
	RRLS-Nys	9.20(0.90)	99.94	99.96(0.00)
	SCRFF	0.46(0.01)	99.93	99.95(0.00)
	LS-RFF	0.56(0.57)	99.93	99.95(0.00)
	Ours	1.12(0.01)	99.94	99.97(0.00)
Covtype n=456,533 m=124,479 d=54	Nys	15.96(0.17)	95.14	97.81(0.03)
	RRLS-Nys	13.85(0.58)	95.13	97.81(0.02)
	SCRFF	4.85(0.39)	95.11	97.80(0.00)
	LS-RFF	6.52(0.11)	95.15	97.80(0.00)
	Ours	3.36(0.07)	95.15	97.81(0.03)

two classes by 4×4 XOR problem. Then we randomly chose 1,000,000 points as training samples and the remaining 600,000 points as test samples.

In order to analyze the influence of the sampling size on the classification performance of the Nys and RRLS-Nys, we gradually increased the sampling size from 100 to 900. Fig. 4 shows the variation of AUC and training time with the sampling size for Nys and RRLS-Nys, respectively.

As can be seen from Fig. 4(a), the performance of the Nys and RRLS-Nys improves with the increase of the sampling size. However, the performance of the Nys and RRLS-Nys cannot be

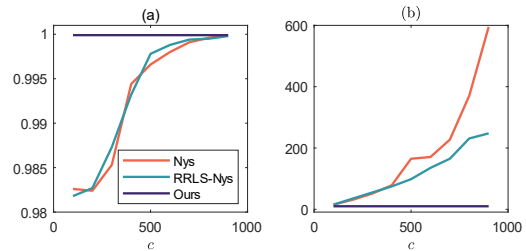


Fig. 4: AUC and training time with different sampling size on the Checkerboard dataset.

comparable to that of our method until the sampling size is 900. In addition, it can be seen from Fig. 4(b) that the training time of Nys and RRLS-Nys increased significantly with the increase of the sampling size, which is much larger than ours. Based on the above analyses, we conclude that our method is more suitable for the Checkerboard dataset.

4.5 Multi-class Classification

In this section, Multi-classification experiments were performed by one-versus-all [48] on the six benchmark multi-classification datasets. In order to compare the performance of the five approximation algorithms objectively and impartially, we also adopted the Macro averaged F1 scores (Macro- F_1) [49] and the Matthews correlation coefficient (MCC) [50] as the evaluation criteria. The detailed information of the six benchmark multi-classification datasets are listed in Table 5. And these datasets were downloaded from the LIBSVM [42].

Table 5: Datasets used in multi-classification experiments.

Data Sets	Train num.	Test num.	Features	Classes
Shuttle	43,500	14,500	9	7
Sensorless	46,656	11,853	48	11
Connect-4	54,872	12,685	126	3
Mnist	60,000	10,000	784	10
Vehicle	78,823	19,705	100	3
CovtypeM	456,533	124,479	54	7

Table 6 reports the experimental results for the six benchmark multi-classification datasets.

From Table 6, it can be clearly seen that our method always has the least time cost, which is consistent with the time complexity. Judging

Table 6: Comparison of different algorithms on the six benchmark multi-classification datasets. The standard deviations are given in brackets.

Data Sets	Algorithms	Training time(s)	Acc (%)	Macro- F_1 (%)	MCC (%)
Shuttle	Nys	5.78(0.10)	99.77	73.81(0.11)	99.35(0.01)
	RRLS-Nys	8.70(0.37)	99.78	74.03(0.50)	99.35(0.01)
	SCRFF	1.81(0.05)	99.77	73.86(0.14)	99.35(0.00)
	LS-RFF	2.27(0.09)	99.78	73.94(0.13)	99.36(0.00)
	Ours	2.39(0.06)	99.77	73.76(0.00)	99.35(0.00)
Sensorless	Nys	9.13(0.06)	98.92	98.91(0.01)	98.81(0.11)
	RRLS-Nys	9.81(0.18)	98.91	98.92(0.01)	98.81(0.11)
	SCRFF	15.19(0.15)	98.90	98.90(0.01)	98.79(0.01)
	LS-RFF	19.37(0.17)	98.93	98.93(0.00)	98.82(0.00)
	Ours	4.18(0.05)	98.91	98.91(0.01)	98.80(0.01)
Connect-4	Nys	1.53(0.03)	80.94	57.55(0.49)	58.63(0.54)
	RRLS-Nys	2.15(0.05)	80.78	57.45(0.55)	58.50(0.73)
	SCRFF	8.60(0.07)	81.16	58.29(0.58)	59.13(0.65)
	LS-RFF	10.90(0.09)	81.31	58.16(0.41)	59.30(0.44)
	Ours	1.33(0.05)	81.71	59.68(0.59)	60.55(0.54)
Mnist	Nys	15.97(0.30)	96.80	96.79(0.00)	96.44(0.00)
	RRLS-Nys	29.24(0.34)	96.80	96.79(0.03)	96.44(0.04)
	SCRFF	97.26(3.09)	96.74	96.74(0.01)	96.38(0.02)
	LS-RFF	122.4(0.56)	96.80	96.80(0.41)	96.45(0.03)
	Ours	8.37(0.16)	96.75	96.74(0.00)	96.39(0.00)
Vehicle	Nys	3.08(0.13)	82.77	82.00(0.01)	72.78(0.01)
	RRLS-Nys	3.57(0.27)	82.80	82.02(0.01)	72.82(0.11)
	SCRFF	16.95(0.10)	82.77	81.98(0.01)	72.76(0.01)
	LS-RFF	20.68(0.18)	82.86	82.09(0.00)	72.92(0.03)
	Ours	1.77(0.05)	82.76	81.98(0.01)	72.76(0.01)
CovtypeM	Nys	110.8(1.85)	94.08	90.25(0.16)	90.49(0.01)
	RRLS-Nys	92.95(1.85)	94.13	90.27(0.16)	90.56(0.12)
	SCRFF	101.1(0.45)	94.06	90.09(0.13)	90.45(0.01)
	LS-RFF	130.4(1.37)	94.07	90.10(0.33)	90.48(0.11)
	Ours	24.21(0.41)	94.09	90.11(0.19)	90.51(0.01)

from different evaluation criteria, the classification performance of the five approximation algorithms is neck and neck. Furthermore, it is clear that the larger the training set, the more significant the speedup of our method. This proves that our method is more effective to solve the multi-classification problem.

5 Conclusion

Kernel Logistic Regression (KLR) has a direct probabilistic interpretation and has good performance in many classification problems. However, the time and space complexity are prohibitive for

large-scale issues. In this paper, we employ multilevel circulant matrix (MCM) approximation to save storage space and accelerate the solution of the KLR. Combined with the characteristics of MCM and our inspiring design, we propose a fast Newton method based on MCM approximation. Because MCM's built-in periodicity allows the multidimensional fast Fourier transform (mFFT) to be used in our method, the time complexity and space complexity of each iteration are reduced to $O(n \log n)$ and $O(n)$, respectively. The experimental results show that our method makes KLR scalable for some large-scale binary and multi-class problems. At the same time, our method provides faster speed and less memory consumption for training. In addition, the experimental results also show that the larger the training set size, the more significant the speedup of our method. Therefore, fast Newton method based on MCM approximation is a more suitable choice for handling large-scale KLR problems.

In this paper, KLR is taken as an example to study the application of MCM in kernel approximation. The kernel approximation method and its Newton equation approximation technique can be used in other kernel learning, such as support vector machines [51, 52, 53], to reduce the storage space and time complexity.

Acknowledgments. This work was supported by the National Natural Science Foundation of China [Grants numbers 61772020].

Declarations

- Data availability statement

Some or all data, models, or code generated or used during the study are available from the corresponding author by request.

References

- [1] Tommi S Jaakkola and David Haussler. Probabilistic kernel regression models. In *Proceedings of the Seventh International Workshop on Artificial Intelligence and Statistics*, pages 94–102, Fort Lauderdale, FL, USA, Jan. 1999.
- [2] Avishek Choudhury. Predicting cancer using supervised machine learning: Mesothelioma.

- Technology and Health Care*, 29(1):45–58, 2021.
- [3] Guijun Yang, Yameng Zhou, Lingli Sun, and Yuhui Shi. Logistic model based on Benford’s law and its application in fraud detection. *Journal of Statistics and Information*, 34(8):50–56, 2019. (in Chinese).
- [4] Haoyuan Hong, Biswajeet Pradhan, Chong Xu, and Dieu Tien Bui. Spatial prediction of landslide hazard at the Yihuang area (China) using two-class kernel logistic regression, alternating decision tree and support vector machines. *Catena*, 100(133):266–281, 2015.
- [5] Ji Zhu and Trevor Hastie. Kernel logistic regression and the import vector machine. *Journal of Computational and Graphical Statistics*, 14(1):185–205, 2005.
- [6] Masashi Sugiyama and Jaak Simm. A computationally-efficient alternative to kernel logistic regression. In *Proceedings of the 2010 IEEE International Workshop on Machine Learning for Signal Processing*, pages 124–129, Kittila, Finland, Aug. 2010.
- [7] S Sathiya Keerthi, KB Duan, Shirish K Shevade, and Aun Neow Poo. A fast dual algorithm for kernel logistic regression. *Machine learning*, 61(1):151–165, 2005.
- [8] Christopher Williams and Matthias Seeger. Using the Nyström method to speed up kernel machines. In *Proceedings of the 13th International Conference on Neural Information Processing Systems*, pages 682–688, Cambridge, MA, Dec. 2001.
- [9] Zijian Lei and Liang Lan. Improved subsampled randomized Hadamard transform for linear SVM. In *Proceedings of the AAAI Conference on Artificial Intelligence*, pages 4519–4526, New York, NY, USA, Feb. 2020.
- [10] Hongjie Jia, Liangjun Wang, and Heping Song. Large-scale spectral clustering with stochastic Nyström approximation. In *International Conference on Intelligent Information Processing*, pages 26–34, 2020.
- [11] Yifan Chen and Yun Yang. Fast statistical leverage score approximation in kernel ridge regression. In *International Conference on Artificial Intelligence and Statistics*, pages 2935–2943, 2021.
- [12] Mu Li, Wei Bi, James T Kwok, and Bao-Liang Lu. Large-scale Nyström kernel matrix approximation using randomized SVD. *IEEE Transactions on Neural Networks and Learning Systems*, 26(1):152–164, 2014.
- [13] Daniele Calandriello, Alessandro Lazaric, and Michal Valko. Analysis of Nyström method with sequential ridge leverage score sampling. In *Proceedings of the Thirty-Second Conference on Uncertainty in Artificial Intelligence*, pages 62–71, New Jersey, USA, Jun. 2016.
- [14] Ahmed Alaoui and Michael W Mahoney. Fast randomized kernel ridge regression with statistical guarantees. In *Proceedings of the 28th International Conference on Neural Information Processing Systems*, pages 775–783, Montreal, Canada, Dec. 2015.
- [15] Cameron Musco and Christopher Musco. Recursive sampling for the Nyström method. In *Proceedings of the 31st International Conference on Neural Information Processing Systems*, pages 3836–3848, Red Hook, NY, USA, Dec. 2017.
- [16] Sanjiv Kumar, Mehryar Mohri, and Ameet Talwalkar. Sampling methods for the Nyström method. *The Journal of Machine Learning Research*, 13(1):981–1006, 2012.
- [17] Alex Gittens and Michael W Mahoney. Revisiting the Nyström method for improved large-scale machine learning. *The Journal of Machine Learning Research*, 17(1):3977–4041, 2016.
- [18] Ali Rahimi and Benjamin Recht. Random features for large-scale kernel machines. In *Proceedings of the 20th International Conference on Neural Information Processing Systems*, pages 1177–1184, Red Hook, NY, USA, Dec. 2007.
- [19] L He, N Ray, Y Guan, and H Zhang. Fast large-scale spectral clustering via explicit feature mapping. *IEEE transactions on cybernetics*, 49(3):1058–1071, 2019.
- [20] Quoc Le, Tamas Sarlos, and Alexander Smola. Fastfood - computing Hilbert space expansions in loglinear time. In *Proceedings of the 30th International Conference on Machine Learning*, pages 244–252, Atlanta, Georgia, USA, Jun. 2013.
- [21] Chang Feng, Qinghua Hu, and Shizhong Liao. Random feature mapping with signed circulant matrix projection. In *Proceedings of the 24th International Joint Conference on Artificial Intelligence*, pages 3490–3496, Buenos

- Aires, Argentina, Jul. 2015.
- [22] Kui Xiong, Herbert H. C. Iu, and Shiyuan Wang. Kernel correntropy conjugate gradient algorithms based on half-quadratic optimization. *IEEE Transactions on Cybernetics*, 51(11):5497–5510, 2020.
- [23] T Dao, C De Sa, and C Ré. Gaussian quadrature for kernel features. *Proceedings of the 31st International Conference on Neural Information Processing Systems*, pages 6109–6119, Dec. 2017.
- [24] M Munkhoeva, Y Kapushev, E Burnaev, and I Oseledets. Quadrature-based features for kernel approximation. In *Proceedings of the 32nd International Conference on Neural Information Processing Systems*, pages 9147–9156, Montréal, Canada, Dec. 2018.
- [25] Zhu Li, Jean-Francois Ton, Dino Oglic, and Dino Sejdic. Towards a unified analysis of random fourier features. *Journal of Machine Learning Research*, 22(108):1–51, 2021.
- [26] Fanghui Liu, Xiaolin Huang, Yudong Chen, and Johan AK Suykens. Random features for kernel approximation: A survey on algorithms, theory, and beyond. *IEEE Transactions on Pattern Analysis and Machine Intelligence*, 2021.
- [27] Guohui Song. *Approximation of kernel matrices in machine learning*. PhD thesis, Department of Mathematics, Syracuse University, Syracuse, NY, USA, 2009.
- [28] Guohui Song and Yuesheng Xu. Approximation of high-dimensional kernel matrices by multilevel circulant matrices. *Journal of Complexity*, 26(4):375–405, 2010.
- [29] Lizhong Ding and Shizhong Liao. Approximate model selection for large scale LSSVM. In *The 3rd Asian Conference on Machine Learning*, pages 165–180, Taoyuan, Taiwan, Nov. 2011.
- [30] Richard E Edwards, Hao Zhang, Lynne E Parker, and Joshua R New. Approximate l -fold cross-validation with least squares SVM and kernel ridge regression. In *Proceedings of the 2013 12th International Conference on Machine Learning and Applications*, pages 58–64, NW Washington, DC, United States, Dec. 2013.
- [31] Lizhong Ding and Shizhong Liao. An approximate approach to automatic kernel selection. *IEEE Transactions on Cybernetics*, 47(3):554–565, 2017.
- [32] Lizhong Ding, Shizhong Liao, Yong Liu, Li Liu, Fan Zhu, Yazhou Yao, Ling Shao, and Xin Gao. Approximate kernel selection via matrix approximation. *IEEE Transactions on Neural Networks and Learning Systems*, 31(11):4881–4891, 2020.
- [33] Rong Yin, Yong Liu, Weiping Wang, and Dan Meng. Sketch kernel ridge regression using circulant matrix: Algorithm and theory. *IEEE Transactions on Neural Networks and Learning Systems*, 31(9):3512–3524, 2019.
- [34] Magnus R Hestenes and Eduard Stiefel. Methods of conjugate gradients for solving linear systems. *Journal of Research of the National Bureau of Standards*, 49(6):409–436, 1952.
- [35] Gavin C Cawley and Nicola LC Talbot. Efficient model selection for kernel logistic regression. In *Proceedings of the 17th International Conference on Pattern Recognition*, pages 439–442, Cambridge, UK, Aug. 2004.
- [36] Bernhard Schölkopf, Ralf Herbrich, and Alex J Smola. A generalized representer theorem. In *International Conference on Computational Learning Theory*, pages 416–426, Amsterdam, The Netherlands, Jul. 2001.
- [37] John E Dennis Jr and Robert B Schnabel. *Numerical Methods for Unconstrained Optimization and Nonlinear Equations*. Prentice-Hall: Englewoods Cliffs, 1983.
- [38] Evgenij E Tyrtyshnikov. A unifying approach to some old and new theorems on distribution and clustering. *Linear Algebra and Its Applications*, 232:1–43, 1996.
- [39] P.J. Davis. *Circulant Matrices*. Wiley, 1979.
- [40] Stephen Boyd, Stephen P Boyd, and Lieven Vandenberghe. *Convex Optimization*. Cambridge university press, 2004.
- [41] Nocedal Jorge and J Wright Stephen. *Numerical Optimization*. Spinger, 2006.
- [42] Chih-Jen Lin Chih-Chung Chang. LIBSVM: a library for support vector machines. <https://www.csie.ntu.edu.tw/~cjlin/libSVM/>, 2011.
- [43] Dheeru Dua and Casey Graff. UCI machine learning repository. <http://archive.ics.uci.edu/ml>, 2017.
- [44] Tin Kam Ho and Eugene M Kleinberg. Building projectable classifiers of arbitrary complexity. In *Proceedings of 13th International*

Conference on Pattern Recognition, pages 880–885, Vienna, Austria, Aug. 1996.

- [45] OL Mangasarian and David R Musicant. Lagrangian support vector machines. *The Journal of Machine Learning Research*, 1(3):161–177, 2001.
- [46] Shuisheng Zhou. Sparse LSSVM in primal using Cholesky factorization for large-scale problems. *IEEE Transactions on Neural Networks and Learning Systems*, 27(4):783–795, 2016.
- [47] Li Chen and Shuisheng Zhou. Sparse algorithm for robust LSSVM in primal space. *Neurocomputing*, 275(C):2880–2891, 2018.
- [48] Vladimir Vapnik. *The Nature of Statistical Learning Theory*. Springer science & business media, 2013.
- [49] Harikrishna Narasimhan, Harish Ramaswamy, Aadirupa Saha, and Shivani Agarwal. Consistent multiclass algorithms for complex performance measures. In *Proceedings of the 32nd International Conference on International Conference on Machine Learning*, pages 2398–2407, Lille France, Jul. 2015.
- [50] Jan Gorodkin. Comparing two K-category assignments by a K-category correlation coefficient. *Computational Biology and Chemistry*, 28(5-6):367–374, 2004.
- [51] Shuisheng Zhou, Jiangtao Cui, Feng Ye, Hongwei Liu, and Qiang Zhu. New smoothing SVM algorithm with tight error bound and efficient reduced techniques. *Computational Optimization and Applications*, 56(3):599–617, 2013.
- [52] Vinod Kumar Chauhan, Kalpana Dahiya, and Anuj Sharma. Problem formulations and solvers in linear SVM: a review. *Artificial Intelligence Review*, 52(2):803–855, 2019.
- [53] Shuisheng Zhou and Wendi Zhou. Unified SVM algorithm based on LS-DC loss. *Machine Learning*, 2021.